Spectroscopic Characterization of YedY: The Role of Sulfur Coordination in a Mo(V) Sulfite Oxidase Family Enzyme Form

ARTICLE *in* JOURNAL OF THE AMERICAN CHEMICAL SOCIETY · NOVEMBER 2009

Impact Factor: 12.11 · DOI: 10.1021/ja903087k · Source: PubMed

5 AUTHORS, INCLUDING:

Jing Yang
University of New Mexico
17 PUBLICATIONS **200** CITATIONS
SEE PROFILE

Richard Adrian Rothery
University of Alberta
74 PUBLICATIONS **2,341** CITATIONS
SEE PROFILE

Joel H Weiner
University of Alberta
191 PUBLICATIONS **6,772** CITATIONS
SEE PROFILE

Published in final edited form as:
J Am Chem Soc. 2009 November 4; 131(43): 15612–15614. doi:10.1021/ja903087k.

Spectroscopic Characterization of YedY: The Role of Sulfur Coordination in a Mo(V) Sulfite Oxidase Family Enzyme Form

Jing Yang[†], **Richard Rothery**[¶], **Joseph Sempombe**[†], **Joel H. Weiner**[¶], and **Martin L. Kirk**[†]

Martin L. Kirk: mkirk@unm.edu

[†]Department of Chemistry and Chemical Biology, The University of New Mexico, Albuquerque NM 87131 USA

[¶]Department of Biochemistry, 474 Medical Science Building, University of Alberta, Edmonton, Alberta, T6G27, CANADA

Abstract

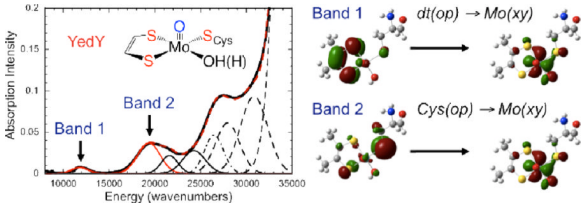

Electronic paramagnetic resonance, electronic absorption, and magnetic circular dichroism spectroscopies have been performed on YedY, a SUOX fold protein with a Mo domain that is remarkably similar to that found in chicken sulfite oxidase, *A. thaliana* plant sulfite oxidase, and the bacterial sulfite dehydrogenase from *S. novella*. Low-energy dithiolene→Mo and cysteine thiolate→Mo charge transfer bands have been assigned for the first time in a Mo(V) form of a SUOX fold protein, and the spectroscopic data have been used to interpret the results of bonding calculations. The analysis shows that second coordination sphere effects modulate dithiolene and cysteine sulfur covalency contributions to the Mo bonding scheme. Namely, a more acute O_{oxo}-Mo-S_{Cys}-C dihedral angle results in increased cysteine thiolate S→Mo charge transfer and a high g_1 in the EPR spectrum. The spectrosocopic results, coupled with the available structural data, indicate that these second coordination sphere effects may play key roles in modulating the active site redox potential, facilitating hole superexchange pathways for electron transfer regeneration, and affecting the type of reactions catalyzed by sulfite oxidase family enzymes.

The pyranopterin molybdenum enzymes are commonly grouped into the sulfite oxidase, DMSO reductase, and xanthine oxidase families based upon the type of reaction they catalyze, their active site structure, and the nature of the overall protein fold.[1] Members of the sulfite oxidase (SO) enzyme family possess a common SUOX protein fold and include vertebrate and plant SO (PSO), the sulfite dehydrogenase from *S. novella* (SDH), assimilatory nitrate reductases, and bacterial YedY.[2] High-resolution crystal structures, coupled with the results of resonance Raman and EPR studies, are consistent with the active site structures shown in Figure 1. The sulfite oxidizing enzymes catalyze the oxidation of sulfite to sulfate, which is the terminal step in the degradation of sulfur containing amino

---

Correspondence to: Joel H. Weiner; Martin L. Kirk, mkirk@unm.edu.

Supporting Information Available: Full Gaussian 03, Inc. reference; details of DFT calculations; molecular orbitals involved in lowest energy LMCT transitions; Table of Mo enzyme spin-Hamiltonian parameters. This material is available free of charge via the Internet at http://pubs.acs.org.

acids and various other sulfur containing chemicals. The catalytic reaction represents a two-electron oxidation of the substrate coupled to an oxygen atom transfer. Under turnover conditions, the paramagnetic Mo(V) form represents an obligatory catalytic intermediate in the electron transfer (ET) regeneration of the catalytically competent active site and is therefore of considerable mechanistic importance. Although the d^1 Mo(V) state in SO family enzymes has been studied extensively by paramagnetic resonance spectroscopies, optical spectroscopies have been extremely limited due to the presence of highly absorbing heme (vertebrate SO and SDH) or the difficulty in preparing high quantities of Mo(V) due to unfavorable Mo(VI)/(V) and Mo(V)/(IV) redox couples (PSO).[3, 4] EPR redox titrations indicate YedY possesses neither of these problems, allowing electronic spectra of a Mo(V) center belonging to an SO family protein to be obtained for the first time.[5]

Very recently the crystal structure of YedY was solved at 2.5Å resolution.[6] The structure revealed that YedY is a monomeric SUOX fold protein with no other cofactors and a Mo domain that is remarkably similar to that found in chicken SO (CSO)[7], *A. thaliana* PSO,[8, 9] and SDH.[10] Furthermore, the coordination geometry of the Mo active site in YedY is virtually identical to that determined for other members of the SO family, although significant differences in the substrate binding pocket, namely the absence of charged arginine residues, suggest that YedY does not effectively bind anionic substrates. The putative reductase activity of YedY is supported by activity assays and kinetic data on a number of oxidizing substrates.[6] Since as-isolated YedY exists primarily in the paramagnetic Mo(V) oxidation state, this allows for detailed spectroscopic probing of the Mo(V) form by a combination of electronic absorption, magnetic circular dichroism, and paramagnetic resonance spectroscopies. The work described here details the first such combined optical and paramagnetic spectroscopic characterization of a Mo(V) SO enzyme form. This provides the basis for correlating EPR derived spin-Hamiltonian parameters, the nature of charge-transfer bands in the electronic spectra, and the active site structure of both YedY and other members of the SO family.

The low temperature (50K) anisotropic X-band EPR spectrum of YedY is presented in Figure 2. Spectral simulations yield spin-Hamiltonian parameters that differ from those reported for SDH, PSO, and CSO.[11–13] Specifically, the g- and A-tensors are highly axial in YedY and a *very* high g_1 is observed. Single crystal EPR studies on mono-oxomolybdenum complexes indicate that the largest primary component of the hyperfine tensor (i.e. A_1) is oriented very close to the Mo≡O bond. For YedY, the non-coincidence angles indicate that g_1 is rotated 19.5° off of A_1 and this is very similar to the 14° and 18° angles found for *hpH* and *lpH* forms of CSO. Although rotations of g_1 relative to A_1 have been correlated to Mo-X (X = F, Cl, Br) bond covalency in C_s symmetry Tp*$MoOX_2$ model compounds[14] no such correlation has been observed in lower symmetry complexes, or the enzymes. The high g_1 for YedY deserves comment as it is even larger than g_1 for the *very rapid* xanthine oxidase intermediate (XO_{vr}).[15] This is important, as XO possesses a terminal sulfido ligand in place of the S_{Cys} donor found in members of the SO family, and the highly covalent $Mo{=}S_{sulfido}$ d-p π^* bonding scheme[16] in XO is believed to be responsible for the high value of g_1 in XO_{vr}. Thus, an increase in Mo(x^2-y^2)-S covalency is the likely origin for the larger g_1 observed in YedY. Both Mo(x^2-y^2)-$S_{dithiolene}$ and Mo(x^2-y^2)-S_{Cys} sulfur covalency contributions are anticipated to increase g_1.[17] We have shown that deviations from an O_{oxo}-Mo-$S_{thiolate}$-C dihedral angle of 90° lead to an increase in Mo(x^2-y^2)-S^v covalency (see Figure 3) in mono-oxo molybdenum thiolate model complexes.[18–20] In contrast, the Mo(x^2-y^2)-S^σ contribution is anticipated to possess a minimal O_{oxo}-Mo-S_{Cys}-C dihedral angle dependence due to the fact that this is a σ bonding interaction. Therefore, second coordination sphere effects in YedY that involve the O_{oxo}-Mo-S_{Cys}-C dihedral angle may lead to the observed increase in g_1 via an increase in the Mo(x^2-y^2)-S^v bonding

interaction.[21] Alternatively, a large dithiolene chelate ring folding about the ligand S---S vector may lead to an increase in g_1.[22–25]

Pink-colored YedY equilibrated in pH = 7 buffer (20 mM MOPS, 500 mM NaCl, and 20 mM Histidine) displays absorption features at 11,825 cm^{-1} (ε = 125 $M^{-1}cm^{-1}$), 19,550 cm^{-1} (ε = 612 $M^{-1}cm^{-1}$), and 27,425 cm^{-1} (ε = 1600 $M^{-1}cm^{-1}$) (Figure 4). Gaussian resolution of the electronic absorption spectrum, coupled with the results of magnetic circular dichroism (MCD) data, provide evidence for a total of at least six electronic transitions below ~30,000 cm^{-1} in YedY. A combination of molecular orbital theory, transition state calculations using time-dependent DFT methods[26, 27] and similarity to spectral features of oxomolybdenum dithiolene and thiolate model complexes have allowed us to understand the electronic origin of the three lowest energy ligand-to-metal charge transfer (LMCT) transitions in YedY.

The highest occupied β molecular orbital (β-HOMO) in oxomolybdenum monodithiolenes is a dithiolene-based MO comprised of two out-of-plane (op), with respect to the dithiolene plane, S atomic orbitals that are in-phase with one-another (S'^{op}; Figure 3). Additionally, the lowest energy acceptor orbital in these complexes is the in-plane (ip) Mo(x^2-y^2) β-LUMO. This acceptor orbital experiences a large stabilization relative to the Mo(xz,yz) orbital set of t_{2g} parentage due to the strong π^* interaction between Mo(xz,yz) orbitals and the terminal oxo ligand.[28] A similar bonding scheme is anticipated for YedY. We therefore assign band 1 as the S'^{op}→Mo(x^2-y^2) LMCT transition (β-HOMO→β-LUMO) based on this MO scheme and the assignment of a similar transition at ~9,000cm^{-1} in Tp*MoO(bdt) (bdt = benzene-1,2-dithiolate) and related complexes.[28] Band 2 is assigned as the cysteine thiolate S^v_{Cys}→Mo(x^2-y^2) transition (β-HOMO-1→β-LUMO) based on spectral assignments in oxomolybdenum thiolate model compounds.[18–20, 29] The orientation of the S^v_{Cys} p orbital is orthogonal to the Mo-S_{Cys} bond, and both the degree of S^v_{Cys}–Mo(x^2-y^2) orbital overlap and the intensity of the S^v_{Cys}→Mo(x^2-y^2) charge transfer transition are related to the O_{oxo}-Mo-S^v_{Cys}-C dihedral angle.[18] We note that the S'^{op}→Mo(x^2-y^2) and S^v_{Cys}→Mo(x^2-y^2) transitions in YedY occur at energies that are ~3,000 cm^{-1} higher than those observed in the model systems. Band 3 is formally the Mo(x^2-y^2)→Mo(xz+yz) ligand-field transition and would be expected to possess a very low oscillator strength. However, due to a large exchange mediated stabilization of the majority spin Mo(x^2-y^2) orbital (α-HOMO-1) there is considerable thiolate character (31% S^v) mixed into the α-HOMO-1 wavefunction.[26, 27] Thus the primary intensity-gaining mechanism is S^v_{Cys}→Mo(xz+yz) and the transition may be thought of as LMCT in nature (α-HOMO-1→α-LUMO+1). A summary of these band assignments is presented in Table 1.

The spectroscopic data on YedY provide insight into how the coordinated dithiolene and cysteine thiolate conspire to modulate the Mo reduction potential and provide a putative hole superexchange pathway for ET regeneration of the dioxomolybdenum (VI) active site in sulfite oxidizing enzymes. The low intensity of the S'^{op}→Mo(x^2-y^2) transition indicates very poor S'^{op}–Mo(x^2-y^2) orbital overlap, which may result from the small amount (~2.5°) of dithiolene chelate ring folding about the S---S vector[22–25] observed in the crystal structure of YedY. Thus, the lack of an appreciable "sulfur fold" effectively decouples the S^{op} dithiolene orbital from the Mo(x^2-y^2) redox orbital. This precludes the involvement of the S'^{op} orbital, either directly or via mixing with the S'^{ip} orbital, in ET processes at this geometry unless ligand redox processes (i.e. the pyranopterin dithiolene) are operative.

The greater intensity of Band 2 indicates an appreciable degree of cysteine thiolate character mixed into the Mo(x^2-y^2) β-LUMO. Our earlier work on oxomolybdenum thiolates[18] indicates that Mo(x^2-y^2)-S^v covalency contributions are minimized when the O_{oxo}-Mo-$S_{thiolate}$-C dihedral angle, *x*, is 90°, and varies as

$$\%S^{v}\text{character}=\cos^2(x) \times (25). \quad \text{Equation 1}$$

Using this expression and the 65° O_{oxo}-Mo-S_{Cys}-C dihedral angle found in YedY, we obtain an estimate of 4.5% S^{v}_{Cys} character in the YedY β LUMO wavefunction, which is in good agreement with what we calculate for the active site by DFT (5.9%).[26, 27]

Although the O_{oxo}-Mo-S_{Cys}-C dihedral angle ranges from 72°–80° in structurally characterized sulfite oxidizing enzymes, their *hpH* and *lpH* g_i values are essentially identical. Thus, in apparent contrast to the structural data, the EPR parameters imply very similar structures for the Mo(V) oxidation state. We have shown that the optimized structure for a computational model of these active sites yields a O_{oxo}-Mo-S_{Cys}-C dihedral angle of 80°,[30] in excellent agreement with the crystallographically determined CSO geometry. According to Eqn. 1, an 80° dihedral angle results in ~0.75% S^{v}_{Cys} character in the CSO β LUMO wavefunction. Thus, the increased value of g_1 and the more acute O_{oxo}-Mo-S_{Cys}-C dihedral angle observed in the structure of YedY strongly support an ~6-fold increase in YedY Mo(x^2-y^2) - S^{v}_{Cys} covalency when compared with Mo(V) forms of CSO, PSO, SDH. Our calculations also indicate that the presence of an aqua ligand, as opposed to a hydroxide, can yield g_1 values greater than 2.0 via an increase in Mo-S covalency. These factors may be at least partially responsible for the increased stability of the Mo(V) state and the observed reductase activity in YedY compared to other sulfite oxidizing enzymes.[6] Additional dithiolene S^{op}-Mo(xz,yz) and cysteine S^{v}-Mo(xz,yz) bonding interactions could further modulate the reduction potential of the active site through anisotropic ligand-to-metal charge donation,[19, 25, 31] and this would be expected to facilitate a decrease in hard-donor stabilization of a di-oxo Mo(VI) active site.

In conclusion, we have made initial spectral assignments for the lowest energy optical transitions in YedY using a combination of electronic absorption, MCD, and EPR spectroscopies. Importantly, the results indicate that the $S^{op}\rightarrow$Mo(x^2-y^2) transition is markedly weaker than the cysteine thiolate→Mo(x^2-y^2) CT, and this reflects dominant cysteine sulfur covalency contributions to the Mo(x^2-y^2) β-LUMO wavefunction at the YedY active site geometry. This is consistent with a minimal folding of the dithiolene chelate ring in YedY and a more acute O_{oxo}-Mo-S_{Cys}-C dihedral angle compared with Mo(V) forms of CSO, PSO, and SDH. The observation of a more acute O_{oxo}-Mo-S_{Cys}-C dihedral angle in YedY results in increased $S^{v}\rightarrow$Mo(x^2-y^2) charge transfer and this is likely the origin of the high g_1 observed in the EPR spectrum of YedY. Since both $S_{Cys}\rightarrow$Mo and $S_{dithiolene}\rightarrow$Mo CT bands are observed in YedY, this will enable relative thiolate and dithiolene covalency contributions to be probed as a function of specific active site mutations and substrate/inhibitor binding, and directly correlated to EPR data. Finally, the spectrosocopic results presented here, coupled with available structural data, indicate that second coordination sphere effects (i.e. dithiolene chelate ring folding, changes in cysteine thiolate dihedral angles, charge differences surrounding the active site, solvent access) may play key roles in modulating the active site redox potential, facilitating ET regeneration, and affecting the type of reactions catalyzed by SO family enzymes.

Supplementary Material

Refer to Web version on PubMed Central for supplementary material.

Acknowledgments

M.L.K. acknowledges support form the National Institutes of Health (Grant No. GM-057378). J.H.W. acknowledges support of from the Canadian Institutes of Health Research (Grant No. MOP15292).

REFERENCES

1. Hille R. Chem. Rev. 1996; 96:2757–2816. [PubMed: 11848841]
2. Workun GJ, Moquin K, Rothery RA, Weiner JH. Microbiology and Molecular Biology Reviews. 2008; 72:228–248. [PubMed: 18535145]
3. Helton ME, Pacheco A, McMaster J, Enemark JH, Kirk ML. J. Inorg. Biochem. 2000; 80:227. [PubMed: 11001093]
4. Jones RM, Inscore FE, Hille R, Kirk ML. Inorg. Chem. 1999; 38:4963. [PubMed: 11671238]
5. Brokx SJ, Rothery RA, Zhang GJ, Ng DP, Weiner JH. Biochemistry. 2005; 44:10339–10348. [PubMed: 16042411]
6. Loschi L, Brokx SJ, Hills TL, Zhang G, Bertero MG, Lovering AL, Weiner JH, Strynadka NCJ. J. Biol. Chem. 2004; 279:50391–50400. [PubMed: 15355966]
7. Kisker C, Schindelin H, Pacheco A, Wehbi WA, Garrett RM, Rajagopalan KV, Enemark JH, Rees DC. Cell. 1997; 91:973–983. [PubMed: 9428520]
8. Hille R. Structure. 2003; 11:1189. [PubMed: 14527382]
9. Schrader N, Fischer K, Theis K, Mendel RR, Schwarz G, Kisker C. Structure. 2003; 11:1251. [PubMed: 14527393]
10. Kappler U, Bailey S. J. Biol. Chem. 2005; 280:24999. [PubMed: 15863498]
11. Kappler U, Bailey S, Feng CJ, Honeychurch MJ, Hanson GR, Bernhardt PV, Tollin G, Enemark JH. Biochemistry. 2006; 45:9696–9705. [PubMed: 16893171]
12. Hemann C, Hood BL, Fulton M, Hansch R, Schwarz G, Mendel RR, Kirk ML, Hille R. J. Am. Chem. Soc. 2005; 127:16567. [PubMed: 16305246]
13. Lamy MT, Gutteridge S, Bray RC. Biochem. J. 1980; 185:397–403. [PubMed: 6249254]
14. Nipales NS, Westmoreland TD. Inorg. Chem. 1997; 36:756–757.
15. Wilson GL, Greenwood RJ, Pilbrow JR, Spence JT, Wedd AG. J. Am. Chem. Soc. 1991; 113:6803–6812.
16. Doonan CJ, Rubie ND, Peariso K, Harris HH, Knottenbelt SZ, George GN, Young CG, Kirk ML. J. Am. Chem. Soc. 2008; 130:55–65. [PubMed: 18062689]
17. Drew SC, Hill JP, Lane I, Hanson GR, Gable RW, Young CG. Inorganic Chemistry. 2007; 46:2373–2387. [PubMed: 17343374]
18. Peariso K, Helton ME, Duesler EN, Shadle SE, Kirk ML. Inorg. Chem. 2007; 46:1259–1267. [PubMed: 17291118]
19. McNaughton RL, Helton ME, Cosper MM, Enemark JH, Kirk ML. Inorg. Chem. 2004; 43:1625–1637. [PubMed: 14989655]
20. McNaughton RL, Tipton AA, Rubie ND, Conry RR, Kirk ML. Inorg. Chem. 2000; 39:5697–5706. [PubMed: 11151370]
21. Peariso K, Chohan BS, Carrano CJ, Kirk ML. Inorg. Chem. 2003; 42:6194–6203. [PubMed: 14514295]
22. Inscore FE, Joshi HK, McElhaney AE, Enemark JH. Inorg. Chim. Acta. 2002; 331:246.
23. Joshi HK, Cooney JJA, Inscore FE, Gruhn NE, Lichtenberger DL, Enemark JH. Proc. Natl. Acad. Sci. U. S. A. 2003; 100:3719. [PubMed: 12655066]
24. Inscore FE, Knottenbelt SZ, Rubie ND, Joshi HK, Kirk ML, Enemark JH. Inorg. Chem. 2006; 45:967. [PubMed: 16441102]
25. Kirk ML, Helton ME, McNaughton RL. Prog. Inorg. Chem. 2004; 52:111–212.
26. Molecular orbitals were analyzed using the AOMix program [a, b]. (a)Gorelsky SI. AOMix: Program for Molecular Orbital Analysis. 1997TorontoYork Universityhttp://www.sh-chem.net/ (b) Gorelsky SI, Lever ABP. J. Organomet. Chem. 2001; 635:187–196.
27. Gaussian 03. Pittsburgh, PA: R. C. G., Inc.; 2003.
28. Inscore FE, McNaughton R, Westcott BL, Helton ME, Jones R, Dhawan IK, Enemark JH, Kirk ML. Inorg. Chem. 1999; 38:1401–1410.
29. McMaster J, Carducci MD, Yang YS, Solomon EI, Enemark JH. Inorg. Chem. 2001; 40:687. [PubMed: 11225111]

30. Peariso K, McNaughton RL, Kirk ML. J. Am. Chem. Soc. 2002; 124:9006–9007. [PubMed: 12148977]

31. Holm RH, Kennepohl P, Solomon EI. Chem. Rev. 1996; 96:2239–2314. [PubMed: 11848828]

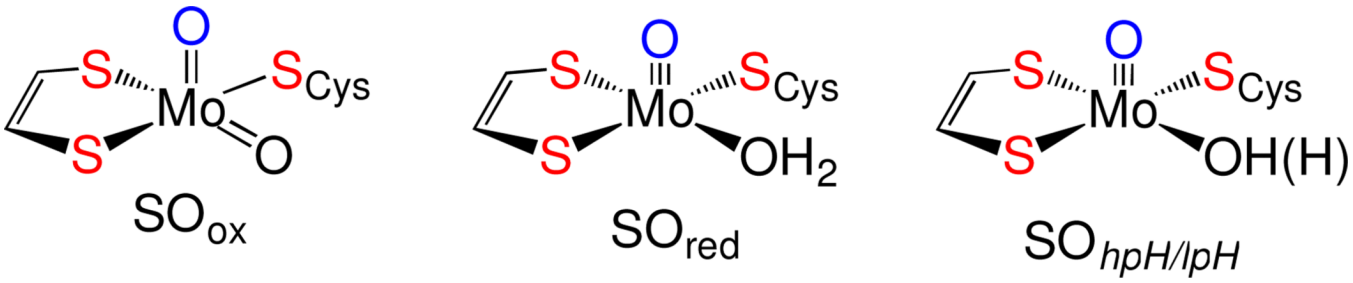

Figure 1.
Accepted oxidized (SO_{ox}), reduced (SO_{red}) and Mo(V) pH dependent ($SO_{hpH/lpH}$) active site structures for SO family enzymes. Note the average O_{oxo}-Mo-S_{Cys}-C dihedral angles are 80° for chicken SO (CSO) and 65° for YedY.

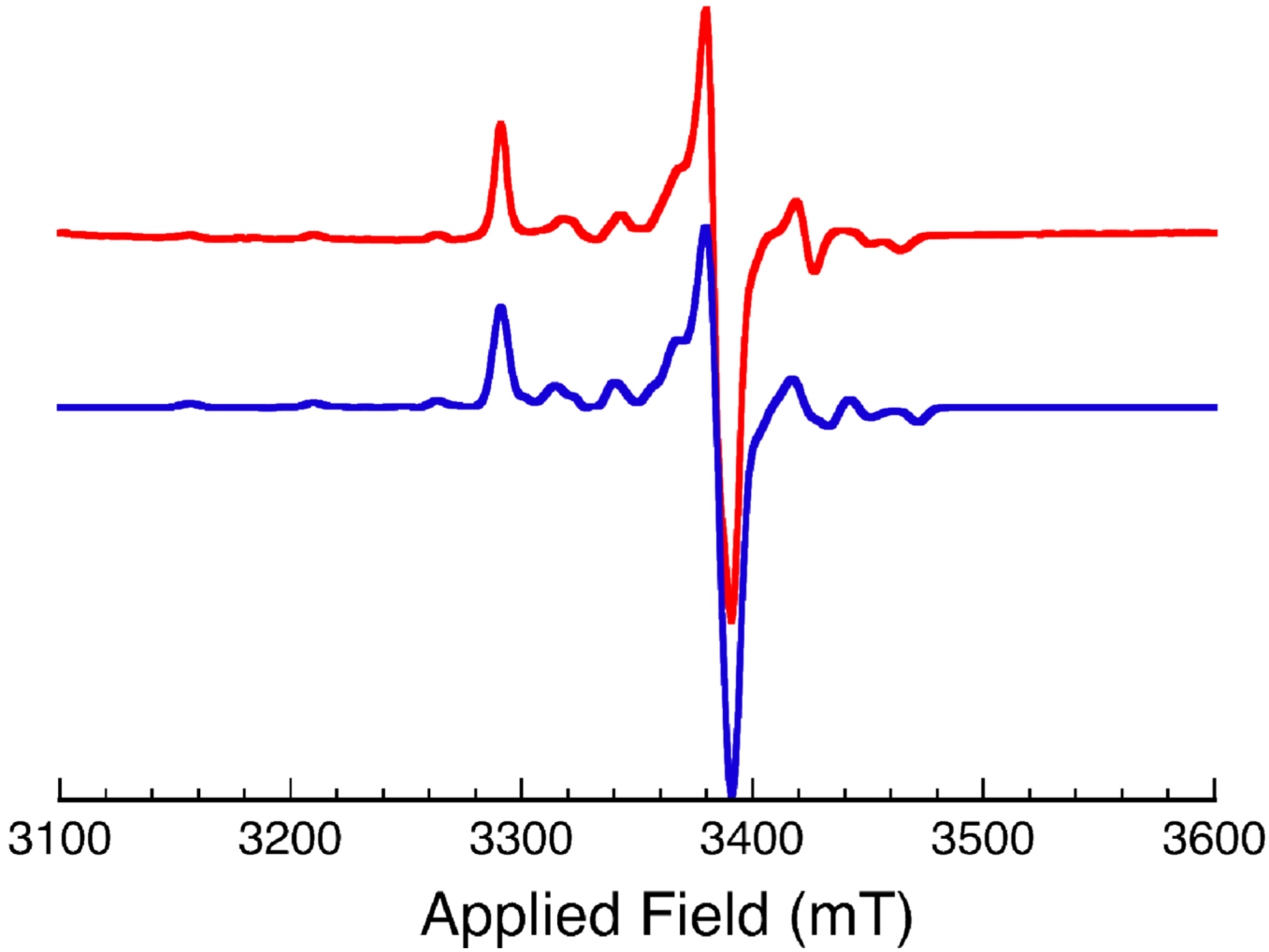

Figure 2.

50 K X-band EPR spectrum of as-isolated YedY (red). Spectral simulation (blue) yields g_1= 2.030, g_2= 1.974, g_3= 1.969, A_1= 54.5×10^{-4} cm^{-1}, A_2= 23.5 ×10^{-4} cm^{-1}, A_3= 22.5 ×10^{-4} cm^{-1}, with Euler angles of α = 35.5°, β = 19.5° and γ = −46.0°. Note that the highly axial nature of the YedY EPR spectrum results in a large degree of uncertainty in α and γ.

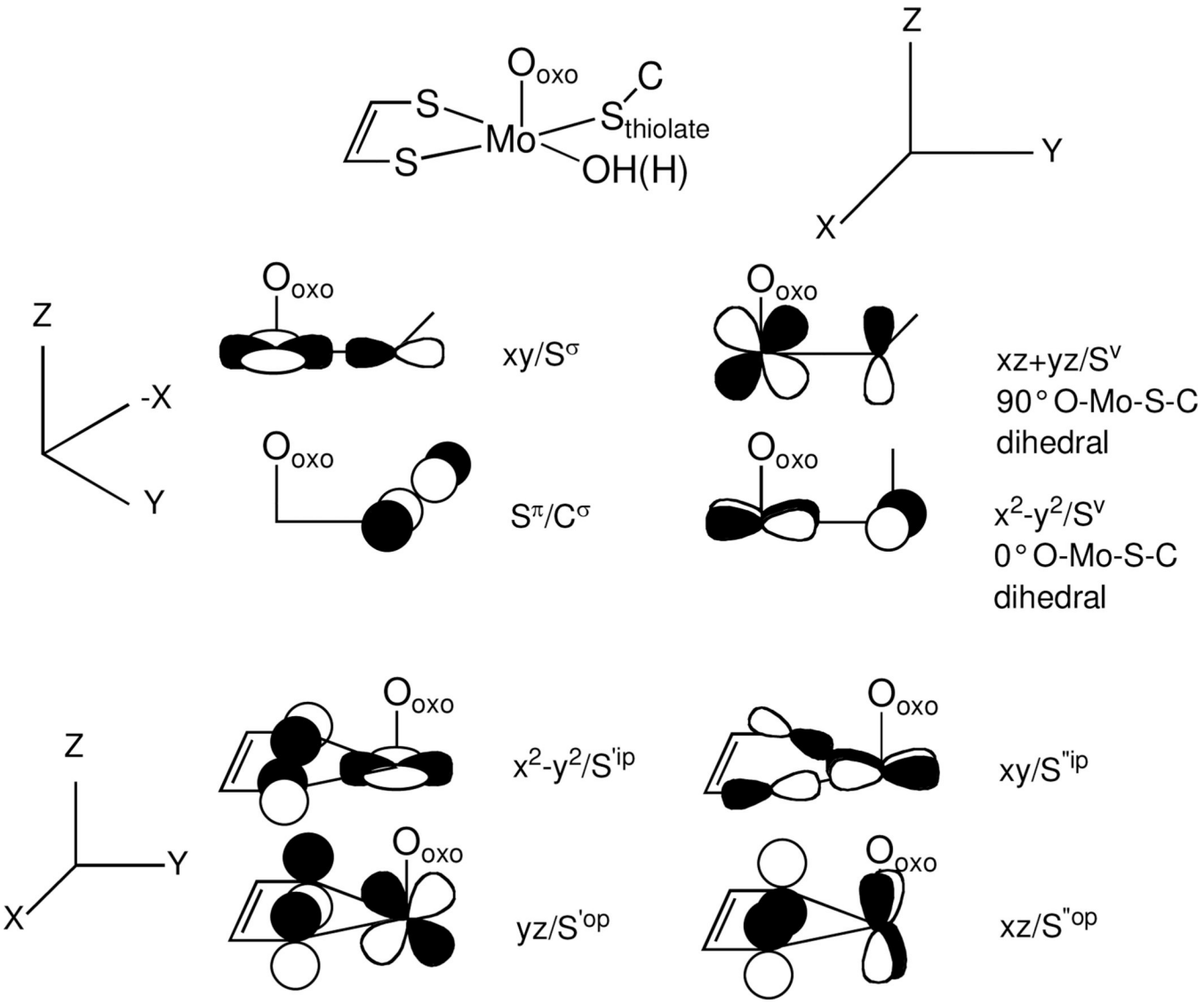

Figure 3.
Symmetrized Mo-thiolate (top) and Mo-dithiolene (bottom) bonding interactions in YedY.

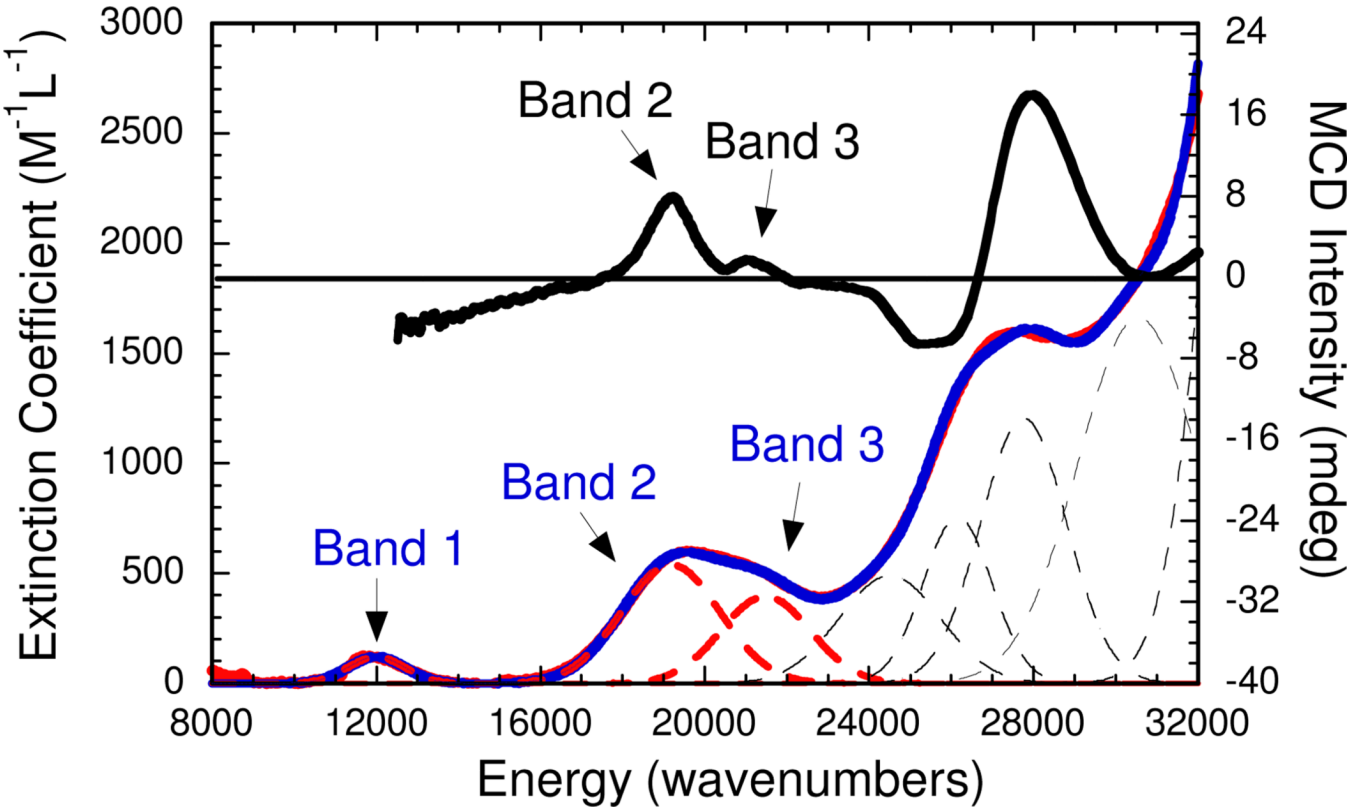

Figure 4.
As isolated YedY MCD at 7T and 5K (black) and electronic absorption spectra at 300K (blue). Guassian resolution of the absorption spectrum is shown as dashed lines and the composite spectrum is presented as a red line.

Table 1

Electronic absorption and MCD band assignments.

Band	$E^{(soln)}_{max}$ (cm^{-1})	Oscillator Strength (exp/calc)	$E^{(MCD)}_{max}$ (cm^{-1})	Assignment
1	11,900	.0009/.0003	n.d.	$S'^{op} \rightarrow Mo(x^2-y^2)$
2	19,122	.0069/.0044	19,289	$S^{v}_{Cys} \rightarrow Mo(x^2-y^2)$
3	21,578	.0047/.0033	21,026	$Mo(x^2-y^2) + S^{v}_{Cys} \rightarrow Mo(xz+yz)$